Research Article

Xiangzhou Hu, Zhijie Yang, Senxian Kang, Man Jiang*, Zuowan Zhou, Jihua Gou, David Hui, and Jing He

Cellulose hydrogel skeleton by extrusion 3D printing of solution

https://doi.org/10.1515/ntrev-2020-0025
Received January 16, 2020; accepted January 24, 2020

Abstract: Cellulose is the most abundant natural polymer on earth, which has obtained increasing interest in the field of functional materials development for its renewable, high mechanical performance and environmental benign. In this study, the traditional processing method (wet spinning and film production) of cellulose-based materials was applied by using cellulose solution for 3D printing, which can directly build complex 3D patterns. Herein, a natural cellulose is dissolved in an effective mixed aqueous solution of dimethyl sulfoxide (DMSO) and tetrabutylammonium hydroxide (TBAH). The cellulose solution extrusion was controlled by a modified fused deposition modeling (FDM) 3D printer. During the controlled extrusion 3D printing process, the viscous cellulose solution will gelifies and further solidifies into a predetermined 3D pattern at room temperature in air. Subsequently, a cellulose hydrogel skeleton was obtained, when the 3D pattern was solvent-exchanged with deionized water. Finally, the mechanical and swelling performance of the cellulose hydrogel scaffold was improved by a cross-linking agent treatment method. With treatment of the 3D printed scaffolds in 0.8 wt% cross-linking agent solution, the obtained cellulose hydrogel could absorb 28 g/g water, and the compression strength was 96 kPa. This work provided an efficient way to prepare natural cellulose hydrogel by 3D printing under room temperature.

Keywords: cellulose, solution, 3D printing, hydrogel skeleton

1 Introduction

3D printing is an important additive manufacturing (AM) method, which can produce complex geometries according to the computer design. During the past years, some revolutionary techniques have been created to realize rapid and scalable 3D printing with high resolution by new stereolithography, tomographic reconstruction techniques [1–3]. The development of the materials in tissue engineering [4–6] provides opportunities for 3D printing, since it is able to construct high precision and complex shapes [7–9]. The 3D bio-printing has also obtained great progress in building components of human organs [10–14]. As a biomass derived natural organic polymer, cellulose has been considered an attractive material for the fabrication of bio-compatible and bio-degradable multifunctional products. But the processes are always complex and time consuming. It is particularly difficult to dissolve the cellulose in common solvents and it cannot be melted with heating. Because of the recalcitrant property, it is difficult to efficiently extract the cellulose, in order to apply it. Hence, the lignocellulose biomass has also been refined into bioethanol and biodiesel by chemical or biological catalysis process [15–17], or been prepared into biomass based carbon materials for supercapacitor electrode [18, 19]. A specific cellulose such as nanocrystal [20–22] or nanofibers cellulose hydrogels [23–25] has been applied for 3D printing to fabricate 3D structures.

*Corresponding Author: Man Jiang, Key Laboratory of Advanced Technologies of Materials (Ministry of Education), School of Materials Science and Engineering, Southwest Jiaotong University, Chengdu, 610031, China; e-mail: jiangman1021@swjtu.edu.cn
Xiangzhou Hu, Zhijie Yang, Senxian Kang, Zuowan Zhou: Key Laboratory of Advanced Technologies of Materials (Ministry of Education), School of Materials Science and Engineering, Southwest Jiaotong University, Chengdu, 610031, China
Jihua Gou: Department of Mechanical and Aerospace Engineering, University of Central Florida, Orlando, FL 32816, United States of America
David Hui: Composite Material Research Laboratory, Department of Mechanical Engineering, University of New Orleans, New Orleans, LA 70148, United States of America
Jing He: Key Laboratory of Development and Application of Rural Renewable Energy, Biogas Institute of Ministry of Agriculture and Rural Affairs, Chengdu 610041, China

The challenges still exist for direct utilization of natural cellulose for 3D printing. Except the stubborn properties of cellulose itself, the obstacle also comes from the work modes of present 3D printer. 3D printer with fused deposition modeling (FDM) is commonly used for thermoplastic polymer filaments 3D printing, such as polylactic acid (PLA) [26–29], acrylonitrile butadiene styrene (ABS) [30–33], and polycarbonate (PC) [34, 35]. Those reactive thermal-setting polymers like epoxy [36, 37] are also applied for 3D printing, cured by irradiation of UV, laser, or heat. Besides, other 3D printers of different work principles include powder bed and ink-jet head 3D printing (3DP), stereolithography (SLA), 3D plotting/direct-write, and selective laser sintering (SLS) has been detailed summarized [38]. In the field of shape memory polymer composite, 3D printing also presents promising advantages for obtaining complicated three-dimensional structures [39–41].

In this work, the mixed aqueous solution consisting of dimethyl sulfoxide and tetrabutylammonium hydroxide (DMSO/TBAH/H_2O) has been adopted as a solvent for natural cellulose. It has been discovered as an outstanding room temperature solvent for cellulose in our previous research [42]. The favorable rheological properties required for 3D printing can be provided by convenient tuning the concentration of the natural cellulose solution. The gelation of the cellulose solution during the extrusion proceeds 3D printing in the air to produce a solid shape, which was then conducted by a solvent exchange with water to obtain the cellulose hydrogel skeleton. Different from the widely used nanocrystal or nanofibril cellulose hydrogel in recent days, a facile procedure is provided to realize the direct 3D printing of natural cellulose viscous solution.

2 Materials and methods

The cotton cellulose was provided by Xinxiang Chemical Fiber Co., Ltd (Henan, China), which was dried at 105°C for 4 hours and smashed into cotton fibers for dissolving. The degree of polymerization (DP) of this cotton cellulose was measured by the gel permeation chromatography (GPC) in our previous work [43] and the result was DP_{GPC} = 731. Dimethyl sulfoxide (DMSO, Mw = 78.13 g·mol^{-1}) purchased from Chengdu Kelong Chemical Reagent Co., Ltd (Sichuan, China) and Tetrabutyl ammonium hydroxide (TBAH, 15wt% aqueous solution) was purchased from Runjing Chemical Co. Ltd (Jiangsu, China), which was condensed into 50wt% under reduced pressure. N, N'-Methylenebisacrylamide (MBA, Mw = 154.17 g·mol^{-1}) was supplied by Chengdu Haihong Chemical Reagent Co., Ltd (Sichuan, China). All chemicals used in this work were of an analytical grade, and were applied without further purification.

2.1 Preparation of viscous cellulose solution

The refined 50wt% TBAH aqueous solution was mixed with DMSO to make the mixed solvent of DMSO/TBAH/H_2O in the weight ratio of 8:1:1. The 6.3 wt% and 6.7 wt% cellulose solutions were prepared by adding the certain amount of cellulose into the solvent under stirring at 1600 rpm for 12 minutes at room temperature into transparent solution. Before 3D printing, the cellulose solution was further conducted with vacuum defoaming treatment.

2.2 3D printing

The 3D printer applied in this work was a modified plastic 3D printer MakerBot Replicator 2X with a solution extruder, which replaced the plastic extruder. The solution extruder was combined with a syringe filled with cellulose solution and was powered by an injection pump. The modified printer is shown in Figure 1. The Simplify 3D software was used to control the printing routes. A CAD file in *stl* mode was converted to a *g* code file to be read by the printer. A nozzle with diameter of 564μm was selected to conduct the printing with an injecting speed of 30 μl/s to match the printing speed of 2 mm/s.

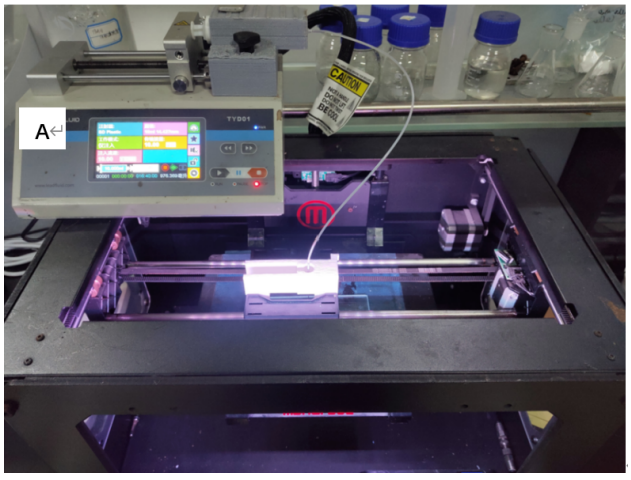

Figure 1: The viscous solution extrusion 3D printer for printing cellulose hydrogel scaffolds. A is the controllable pump fixed with a syringe and needle to pipe out the cellulose solution by extrusion

2.3 Processing of cellulose hydrogel scaffolds

The 6.7 wt% cellulose solution was adopted for the 3D printing. The 3D printed scaffold was put into deionized water (DI water) to conduct solvent exchange to obtain the cellulose hydrogel scaffold. For improving the re-swellability of the 3D printed scaffold, before the solvent exchange in DI water, the 3D printed scaffold was kept in the MBA/DMSO solution with different concentrations for 12 hours at 50°C to form chemical cross-linkage inside the cellulose scaffold. The final 3D printed cellulose hydrogel scaffolds were freeze-dried to observe the morphology by SEM.

3 Characterization

3.1 The rheological property analysis

To find out the suitable concentration of the cellulose solution for 3D printing, the rheological behavior was studied. The rheological property was tested by a Control Stress Rheometer (TA instruments, America). The viscosity of the cellulose solution was measured in steady state with the shear rate ranging from 0 to 100 s^{-1}. To test the storage moduli (G′) and loss moduli (G″), a logarithmic stress sweep was plotted at a frequency of 1 Hz. The frequency sweep was performed in the range from 0 to 100 Hz, at a constant strain rate of 1%. This strain rate was chosen after performing the linear viscoelastic region sweep.

3.2 Chemical structure characterization

To analyze the interactions between the functional groups of the components consisted in the hydrogel scaffolds, with and without crosslink agent treatment, Fourier transform infrared spectroscopy (FT-IR) was recorded on a FT-IR spectrometer equipped with ATR accessory (Nicolet 6700, Nicolet, America). The spectra were recorded in hydrogel samples with a resolution of 4 cm^{-1} and an accumulation of 50 scans in the spectral range of 400-4000 cm^{-1} at room temperature.

3.3 Morphology analysis

The morphology of the freeze-dried 3D printed hydrogel scaffolds was studied with a scanning electron microscope (QUANPA200, FEI, Holland). To observe the morphology of cross section part of the scaffolds, which were dipped in liquid N_2 before cutting. All the samples were coated with gold powder by spraying for 60 seconds at 10 mA.

3.4 The aggregation structure analysis

To compare the aggregation structures with and without crosslinking treatment of the 3D printed scaffolds, the XRD was performed on a X-ray diffractometer (X'pert PRO, PAN alytical, Holland) with copper radiation (λ = 0.154056 nm). The scan range was from 5 to 60°, with a scanning speed of 10°/min.

3.5 Mechanical properties

To evaluate the mechanical properties of the cellulose hydrogel scaffolds, the compression tests were performed on an electronic universal testing machine (CMT4000, Sansitaijie, China) with a compressing speed of 5 m/min. The average value of five samples was taken as the final result.

3.6 Re-swelling performance

The re-swelling performance of cellulose hydrogel scaffolds was evaluated by drying the samples and then dipping into DI water to swell, and calculate the swelling ration (SR) using the Eq. (1),

$$SR(\%) = (Ws - W_d)/W_d \cdot 100\% \quad (1)$$

where Ws is the wet weight of hydrogel after absorbing DI water to a swelling balance, and W_d is the weight of the dried 3D printed cellulose scaffolds. The average value of three testing results was taken as the final result.

4 Results and discussion

4.1 The rheological property of the cellulose solution

The rheological properties of cellulose solutions were tested, and the results were collected in Figure 2. As shown in Figure 2a, the 6.7 wt% cellulose solution appeared as a semisolid. The rheological properties of the cellulose solutions under different temperatures (Figure 2b, 6.7 wt% cellulose solution) and with different concentrations (Figure 2c, 20°C) were tested separately as a function of shear

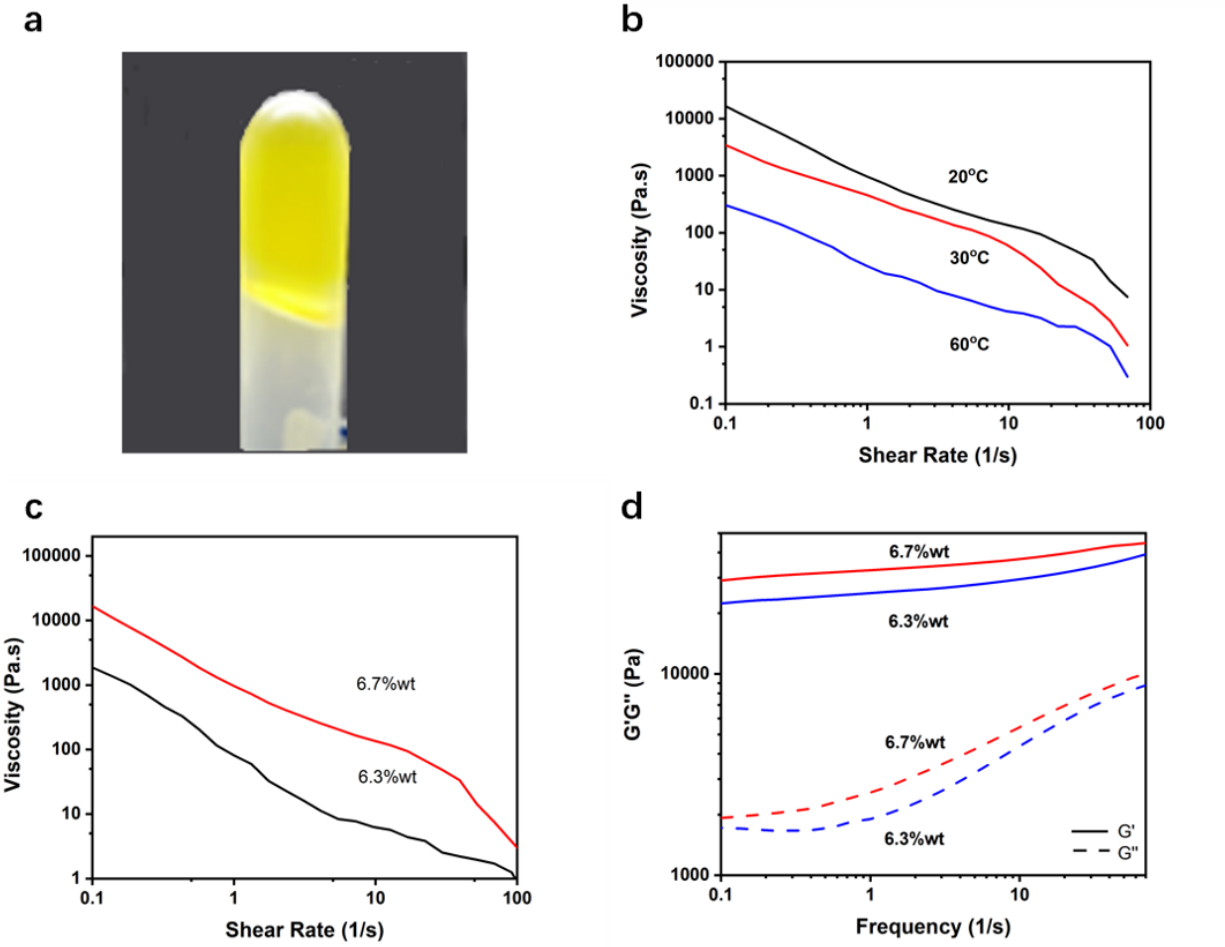

Figure 2: The rheological properties of the viscous cellulose solutions: (a) optical picture of the 6.7 wt% cellulose solution; (b) the viscosity of the 6.7 wt% cellulose solution as a function of shear rate under different temperatures; (c) the viscosity of the cellulose solutions with different concentrations (6.3 wt% and 6.7 wt%) as a function of shear rate; (d) the storage modulus (G′, the hard line) and the loss modulus (G″, the dotted line) of the cellulose solutions with different concentrations (6.3 wt% and 6.7 wt%) under room temperature

rate. With the increasing of the shear rate, the viscosity of the cellulose solution decreased obviously, which presented a strong non-Newtonian shear thinning behavior. The characteristics of the viscous cellulose solution was beneficial for the extrusion 3D printing under room temperature. They were easy to be extruded out through the printing nozzle and then changed into solid-like to form a prescribed shape. As summarized in the Figure 2c, the solid lines, presented the storage modulus (G′), were above the loss modulus (G″) within measuring range. The rheological behavior of the cellulose solution was more like a solid, so they were suitable for conducting 3D printing under room temperature. It could be explained that the entanglement force and hydrogen bond between molecular chains decreased, and the molecular chains would move easily with increasing the shear rate. In the meantime, with increasing the temperature, more free volume would be produced for the molecular chains to move easier. Such rheological properties of the cellulose viscous solutions provided the necessities their 3D printing to keep the stable dimension and precise shape.

4.2 The morphology of the 3D printed cellulose hydrogel scaffolds

The 6.7 wt% cellulose solution was applied for the 3D printing under room temperature. The 3D printed scaffolds were immersed in DI water to conduct regeneration and solvent exchange to produce the aim cellulose hydrogel scaffolds, as shown in Figure 3. As it could been seen that the 3D printed scaffolds, both the as printed samples (a and b) and the hydrogels (a_1 and b_1) after solvent exchange with DI water kept the prescribed shape according

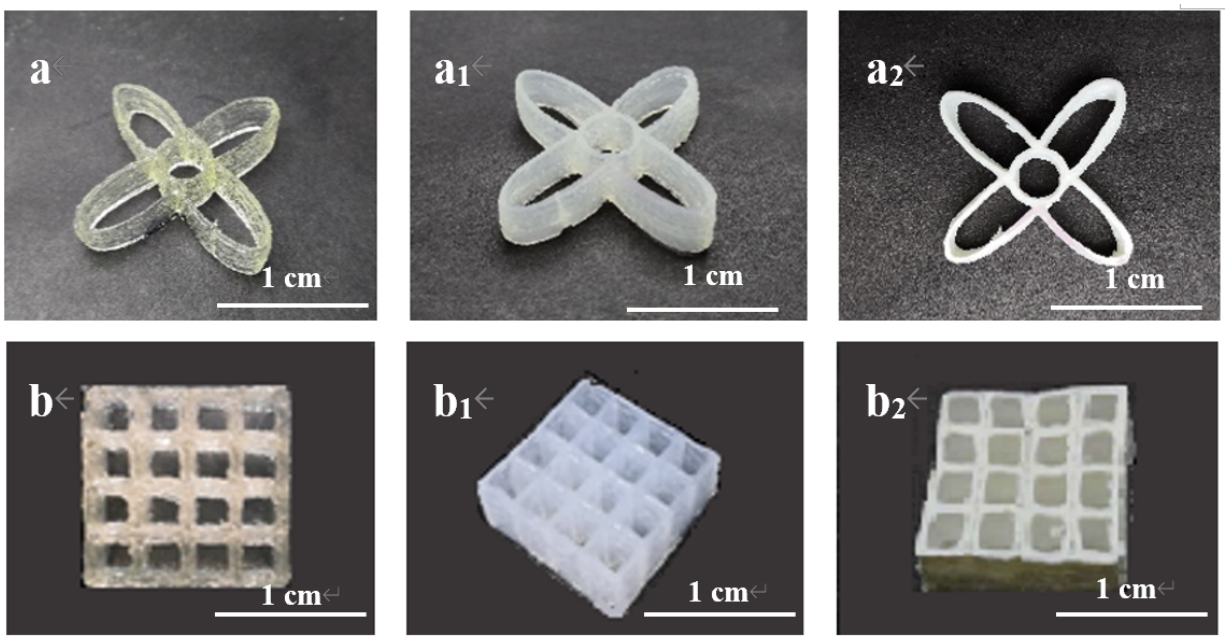

Figure 3: The digital pictures of the 3D printed cellulose scaffolds: a, b – as-printed samples; a_1, b_1 – the hydrogel scaffolds; a_2, b_2 – the freeze-dried samples

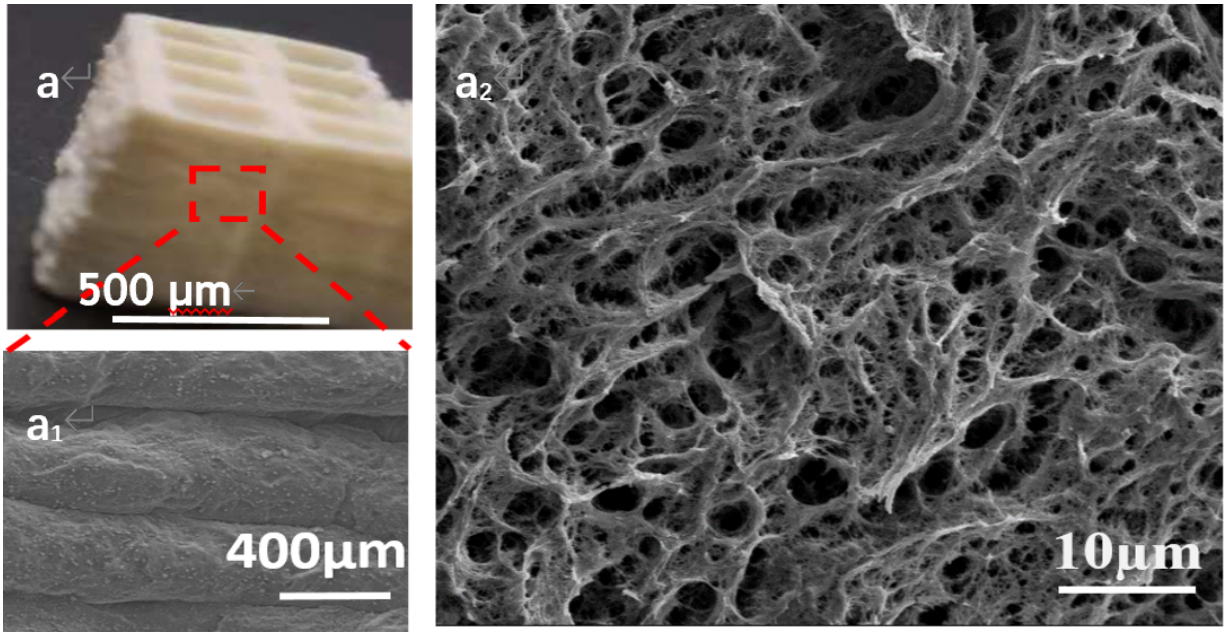

Figure 4: SEM images of the freeze-dried 3D printed cellulose scaffold: (a) the layer by layer printed 3D grid shape; (a_1) the morphology of the surface of the layers; (a_2) the cross section

to the designed CAD models. While, the freeze-dried samples (a_2 and b_2) showed some shrinkage.

In order to take observation into the morphology of the layer by layer printed 3D cellulose scaffolds, the SEM was applied, the images were shown in Figure 4. As shown in Figure 4a and 4b, the side view presented apparent layer by layer stacked structure. The cross section was shown in Figure a_2, the regenerated cellulose fibers in different diameters agglomerated and formed hierarchical pores, which contributed micro and macro chambers to contain water.

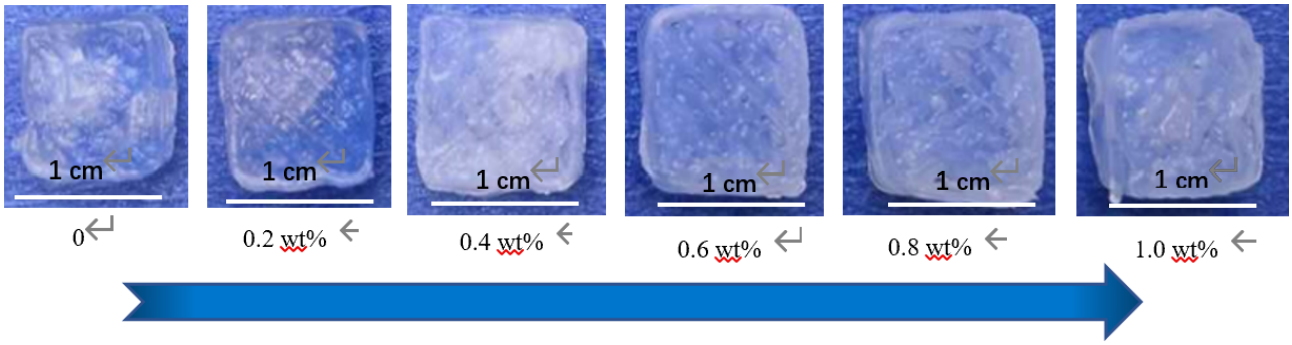

Figure 5: The re-swelled 3D printed cellulose hydrogel samples treated by cross linking agent solutions with different concentrations

Table 1: The re-swelling property of the 3D printed cellulose hydrogel scaffolds treated by MBA/DMSO solution.

MBA content (wt%)	0	0.2	0.4	0.6	0.8	1.0
RS (g/g)	14	19	22	24	28	26

4.3 The impact of the crosslinking agent treatment on the properties of the 3D printed cellulose hydrogel scaffolds

The re-swelling ability is one of the most important property for hydrogel materials. While, the re-swelling ratio of the as prepared cellulose hydrogel scaffold is only 14 wt%. To improve the re-swelling ability, the crosslinking agent (N, N'-Methylenebisacrylamide, MBA) was introduced into the 3D printed cellulose hydrogel scaffolds, by immersing the printed cellulose scaffolds into the MBA/DMSO solution with concentrations ranging from 0 to 1.0 wt%. The pictures of the re-swelled samples were shown in Figure 5. The sample treated in the 0.8 wt% cross link agent solution had the best re-swelling property, which adsorbed 28 g/g DI water of its own weight. With increasing the concentration of the MBA content to 1.0%, the re-swelling ability of the 3D printed cellulose hydrogel decreased to 24 g/g. The re-swelling results of the samples treated by MBA/DMSO solution with different concentrations were summarized in Table 1, and the photos were shown in Figure 5.

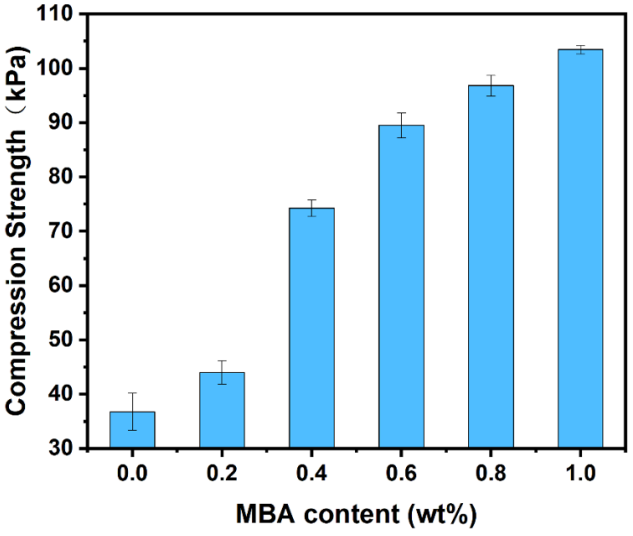

Figure 6: The compression strength of the cross-linking agent treated cellulose hydrogel scaffolds

4.4 The compression properties of the cross-linking agent treated 3D printed cellulose hydrogel scaffolds

The mechanical property is important for the practical utilization of the hydrogel materials, which has also been tested, taking the reported method [44] as reference. As shown in Figure 6, with increasing the concentration of the MBA in the solution, the compression strength was increased from 36 to 103 kPa. Especially, the compression strength considerably increased from 45 to 75 kPa when the concentration of MBA in the cross-linking medium increased from 0.4 to 0.6 wt%.

4.5 Chemical structure analysis by FTIR spectra

In order to understand the interact of the cross-linking agent with the cellulose, the MBA treated cellulose hydrogel scaffolds were freeze dried and analyzed by FTIR, as shown in Figure 7.

The strong adsorption at 1662 and 1627 cm^{-1}, ascribed to the stretching vibration of C=C and C=O in MBA, respec-

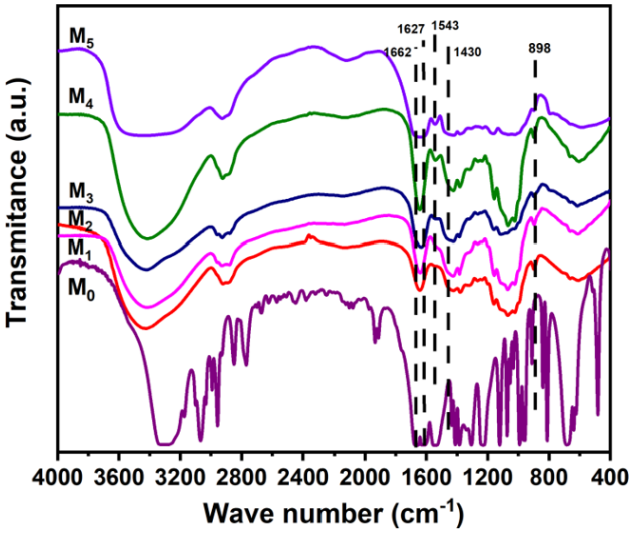

Figure 7: FTIR spectra of the cross-linking agent treated cellulose hydrogel scaffolds. M_0: the MBA, M_1-M_5: the cellulose hydrogel scaffolds treated with 0.2, 0.4, 0.6, 0.8, and 1.0 wt% MBA solutions, respectively

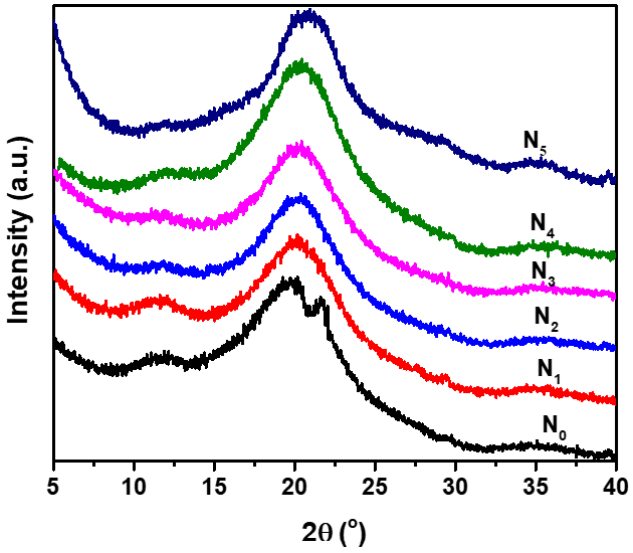

Figure 8: XRD patterns of the cross-linking agent treated cellulose scaffolds. N_0-N_5 corresponding to the cellulose scaffolds treated with 0, 0.2, 0.4, 0.6, 0.8, 1.0 wt% MBA solutions, respectively

tively. The peak at 1543 cm^{-1} and 1430 cm^{-1} represented to the bending vibration of N-H and C-N in MBA [44]. Those typical vibrations presented amide structure of MBA. As shown in the M_1-M_5 of Figure 7, with the increasing of the MBA in the cross-linking agent solution, the representative adsorptions at 1543 cm^{-1} and 1430 cm^{-1} became enhanced. The characteristic adsorption of β-1,4-D-glycosidic bond in cellulose at 897 cm^{-1} were obvious in the M_1-M_5 of Figure 7. Additionally, with the introduction of cross-link agent, the stretching vibration in about 3400 cm^{-1} became wider and some red shift, which indicated the hydrogen bonds formed between the carbonyl groups of MBA and the hydroxyl groups of cellulose. As a result, the MBA was successfully introduced into the cellulose scaffolds.

4.6 The crystal structure analysis by XRD diffraction

The cross-linking agent treated cellulose scaffolds were freeze dried to conduct the XRD analysis to study the effect of the MBA on the crystal structures of cellulose, as shown in Figure 8.

According to the XRD diffraction patterns in Figure 8, with the increase of MBA content in the cross-linking solution, the diffraction peaks of the cellulose in the 110 and 200 crystal planes decreased in intensity, while the $1\bar{1}0$ crystal plane gradually disappeared. As mentioned before, the cross-linking interaction between cellulose and MBA consumed the -OH at C6 in cellulose, which caused the decrease of hydrogen bonds, and hence decreased the crystallinity.

5 Conclusion

In summary, the natural cotton cellulose solution in dimethyl sulfoxide and tetrabutylammonium hydroxide aqueous solution (DMSO/TBAH/H_2O) was found to be suitable for extrusion 3D printing for its special rheological properties. It presented solid-like behavior under room temperature, and a strong non-Newtonian shear thinning property. With introduction of N, N'-Methylenebisacrylamide (MBA) into the 3D printed cellulose hydrogel scaffolds, the compression as well as the re-swelling properties were considerably improved. This work provides a new way for construct complex cellulose hydrogel scaffolds for practical application by 3D printing.

Acknowledgement: The authors acknowledge the financial support from the International Cooperation Project of Sichuan Province (NO.2018HH0087) and the Sichuan Major Science and Technology Project (NO.2019ZDZX0018).

References

[1] Kelly BE, Bhattacharya I, Heidari H, Shusteff M, Spadaccini CM, Taylor HK. Volumetric additive manufacturing via tomographic reconstruction. Science. 2019 Mar;363(6431):1075–9.

[2] Saha SK, Wang D, Nguyen VH, Chang Y, Oakdale JS, Chen SC. Scalable submicrometer additive manufacturing. Science. 2019 Oct;366(6461):105–9.
[3] Walker DA, Hedrick JL, Mirkin CA. Rapid, large-volume, thermally controlled 3D printing using a mobile liquid interface. Science. 2019 Oct;366(6463):360–4.
[4] Kelly CN, Miller AT, Hollister SJ, Guldberg RE, Gall K. Design and Structure-Function Characterization of 3D Printed Synthetic Porous Biomaterials for Tissue Engineering. Adv Healthc Mater. 2018 Apr;7(7):e1701095.
[5] Li RQ, McCarthy A, Zhang YS, Xie JW. Decorating 3D Printed Scaffolds with Electrospun Nanofiber Segments for Tissue Engineering. Adv. Biosys. 2019;3(12):1900137.
[6] Richards DJ, Tan Y, Jia J, Yao H, Mei Y. 3D Printing for Tissue Engineering. Isr J Chem. 2013 Oct;53(9-10):805–14.
[7] Pearre BW, Michas C, Tsang JM, Gardner TJ, Otchy TM. Fast micron-scale 3D printing with a resonant-scanning two-photon microscope. Addit. Manuf. 2019;30:100887.
[8] Kalms M, Narita R, Thomy C, Vollertsen F, Bergmann RB. New approach to evaluate 3D laser printed parts in powder bed fusion-based additive manufacturing in-line within closed space. Addit. Manuf. 2019;26:161–5.
[9] Gelber MK, Hurst G, Comi TJ, Bhargava R. Model-guided design and characterization of a high-precision 3D printing process for carbohydrate glass. Addit. Manuf. 2018;22:38–50.
[10] Grigoryan B, Paulsen SJ, Corbett DC, Sazer DW, Fortin CL, Zaita AJ, et al. Multivascular networks and functional intravascular topologies within biocompatible hydrogels. Science. 2019 May;364(6439):458–64.
[11] Lee A, Hudson AR, Shiwarski DJ, Tashman JW, Hinton TJ, Yerneni S, et al. 3D bioprinting of collagen to rebuild components of the human heart. Science. 2019 Aug;365(6452):482–7.
[12] Bose S, Vahabzadeh S, Bandyopadhyay A. Bone tissue engineering using 3D printing. Mater Today. 2013;16(12):496–504.
[13] Murphy SV, Atala A. 3D bioprinting of tissues and organs. Nat Biotechnol. 2014 Aug;32(8):773–85.
[14] Mannoor MS, Jiang Z, James T, Kong YL, Malatesta KA, Soboyejo WO, et al. 3D printed bionic ears. Nano Lett. 2013 Jun;13(6):2634–9.
[15] Rai M, dos Santos JC, Soler MF, Marcelino PR, Brumano LP, Ingle AP, et al. Strategic role of nanotechnology for production of bioethanol and biodiesel. Nanotechnol Rev. 2016;5(2):231–50.
[16] Lemée L, Kpogbemabou D, Pinard L, Beauchet R, Laduranty J. Biological pretreatment for production of lignocellulosic biofuel. Bioresour Technol. 2012 Aug;117:234–41.
[17] Zhao X, Luo K, Zhang Y, Zheng Z, Cai Y, Wen B, et al. Improving the methane yield of maize straw: focus on the effects of pretreatment with fungi and their secreted enzymes combined with sodium hydroxide. Bioresour Technol. 2018 Feb;250:204–13.
[18] Li ZH, Xu K, Pan YS. Recent development of Supercapacitor Electrode Based on Carbon Materials. Nanotechnol Rev. 2019;8(1):35–49.
[19] Gao T, Xu C, Li R, Zhang R, Wang B, Jiang X, et al. Biomass-Derived Carbon Paper to Sandwich Magnetite Anode for Long-Life Li-Ion Battery. ACS Nano. 2019 Oct;13(10):11901–11.
[20] Sultan S, Mathew AP. 3D printed scaffolds with gradient porosity based on a cellulose nanocrystal hydrogel. Nanoscale. 2018 Mar;10(9):4421–31.
[21] Li VC, Kuang X, Hamel CM, Roach D, Deng YL, Qi HJ. Cellulose nanocrystals support material for 3D printing complexly shaped structures via multi-materials-multi-methods printing. Addit. Manuf. 2019;28:14–22.
[22] Hausmann MK, Rühs PA, Siqueira G, Läuger J, Zimmermann T, Studart AR. 3D printed cellulose nanocrystal composites through digital light processing. ACS Nano. 2018;12(7):6926–37.
[23] Hakansson KM, Henriksson IC, Vazquez CD, Kuzmenko V, Markstedt K, Enoksson P, et al. Solidification of 3D Printed Nanofibril Hydrogels into Functional 3D Cellulose Structures, Adv. Mater Technol. 2016;1(7):1600096.
[24] Xu C, Zhang Molino B, Wang X, Cheng F, Xu W, Molino P, et al. 3D printing of nanocellulose hydrogel scaffolds with tunable mechanical strength towards wound healing application. J Mater Chem B Mater Biol Med. 2018 Nov;6(43):7066–75.
[25] Huang L, Du X, Fan S, Yang G, Shao H, Li D, et al. Bacterial cellulose nanofibers promote stress and fidelity of 3D-printed silk based hydrogel scaffold with hierarchical pores. Carbohydr Polym. 2019 Oct;221:146–56.
[26] Giordano RA, Wu BM, Borland SW, Cima LG, Sachs EM, Cima MJ. Mechanical properties of dense polylactic acid structures fabricated by three dimensional printing. J Biomater Sci Polym Ed. 1996;8(1):63–75.
[27] Kiendl J, Gao C. Controlling toughness and strength of FDM 3D-printed PLA components through the raster layup, Compos. Pt. B-Eng. 2020;180:107562.
[28] Kaygusuz B, Ozerinc S. Improving the ductility of polylactic acid parts produced by fused deposition modeling through polyhydroxyalkanoate additions. J Appl Polym Sci. 2019;136(43):48154.
[29] Tian XY, Liu TF, Wang QR, Dilmurat A, Li DC, Ziegmann G. Recycling and remanufacturing of 3D printed continuous carbon fiber reinforced PLA composites. J Clean Prod. 2017;142(4):1609–18.
[30] Torrado AR, Shemelya CM, English JD, Lin YR, Wicker RB, Roberson DA. Characterizing the effect of additives to ABS on the mechanical property anisotropy of specimens fabricated by material extrusion 3D printing. Addit. Manuf. 2015;6:16–29.
[31] Dilberoglu UM, Simsek S, Yaman U. Shrinkage compensation approach proposed for ABS material in FDM process. Mater Manuf Process. 2019;34(9):993–8.
[32] Samykano M, Selvamani SK, Kadirgama K, Ngui WK, Kanagaraj G, Sudhakar K. Mechanical property of FDM printed ABS: influence of printing parameters. Int J Adv Manuf Technol. 2019;102(9-12):2779–96.
[33] Levenhagen NP, Dadmun MD. Improving Interlayer Adhesion in 3D Printing with Surface Segregating Additives: Improving the Isotropy of Acrylonitrile-Butadiene-Styrene Parts. ACS Appl. Polym. Mater. 2019;1(4):876–84.
[34] Park SJ, Lee JE, Park JH, Lyu MY, Park K, Koo MS, et al. FDM 3D Printing of Environmental Friendly and High Strength Bio-based PC Filaments for Baby Toys. Elastom. Compos. 2017;52(2):99–104.
[35] Yap YL, Toh W, Koneru R, Lin KH, Yeoh KM, Lim CM, et al. A non-destructive experimental-cum-numerical methodology for the characterization of 3D-printed materials-polycarbonate-acrylonitrile butadiene styrene (PC-ABS). Mech Mater. 2019;132:121–33.
[36] Shi Q, Yu K, Kuang X, Mu XM, Dunn CK, Dunn ML, et al. Recyclable 3D printing of vitrimer epoxy. Mater Horiz. 2017;4(4):598–607.
[37] Pierson HA, Celik E, Abbott A, De Jarnette H, Gutierrez LS, Johnson K, et al. Mechanical Properties of Printed Epoxy-Carbon Fiber Composites. Exp Mech. 2019;59(6):843–57.

[38] Wang X, Jiang M, Zhou ZW, Gou JH, Hui D. 3D printing of polymer matrix composites: A review and prospective, Compos. Pt. B-Eng. 2017;110:442–58.
[39] Lei M, Chen Z, Lu HB, Yu K. Recent progress in shape memory polymer composites: methods, properties, applications and prospects. Nanotechnol Rev. 2019;8(1):327–51.
[40] Yang H, Leow WR, Wang T, Wang J, Yu J, He K, et al. 3D Printed Photoresponsive Devices Based on Shape Memory Composites. Adv Mater. 2017 Sep;29(33):1701627.
[41] Wu W, Ye W, Wu Z, Geng P, Wang Y, Zhao J. Influence of Layer Thickness, Raster Angle, Deformation Temperature and Recovery Temperature on the Shape-Memory Effect of 3D-Printed Polylactic Acid Samples. Materials (Basel). 2017 Aug;10(8):E970.
[42] Cao J, Wei W, Gou GJ, Jiang M, Cui YH, Zhang SL, et al. Cellulose films from the aqueous DMSO/TBAH-system. Cellulose. 2018;25(3):1975–86.
[43] Bu D, Hu X, Yang Z, Yang X, Wei W, Jiang M, et al. Elucidation of the Relationship between Intrinsic Viscosity and Molecular Weight of Cellulose Dissolved in Tetra-N-Butyl Ammonium Hydroxide/Dimethyl Sulfoxide. Polymers (Basel). 2019 Oct;11(10):E1605.
[44] Geng H. A one-step approach to make cellulose-based hydrogels of various transparency and swelling degrees. Carbohydr Polym. 2018 Apr;186:208–16.